High Current Hollow Cathode for the X3 100-kW Class Nested Hall Thruster

IEPC-2019-371

Presented at the 36th International Electric Propulsion Conference
University of Vienna • Vienna, Austria
September 15-20, 2019

Giulia Becatti[1], Dan M. Goebel[2], Camilla V. Yoke[3], Alejandro L. Ortega[4], Ioannis G. Mikellides[5]
Jet Propulsion Laboratory, California Institute of Technology, Pasadena, Ca, 91109, USA

Abstract: NASA continues to develop higher power ion and Hall thrusters to provide higher thrust and specific impulse for deep space human and robotic missions. The efforts of the NASA NextSTEP program led to the successful demonstration the XR-100 high power nested Hall thruster system, capable of operating in the 20-200kW power range. The hollow cathode for this thruster is required to produce 50-350A of discharge current with lifetime in excess of 10 khrs. A high-current lanthanum hexaboride hollow cathode has been developed at JPL and was previously tested at discharge currents up to 250A both in the cathode test facility and in the XR-100 thruster. The cathode design has been updated to sustain the higher current demands, and it has currently demonstrated operation at discharge currents up to 330A. The cathode operation has been simulated with the OrCa2D code developed at JPL during the past 15 years. The simulation results are found to be in excellent agreement with measured plasma parameters both inside cathode and in the plume region, at different operating conditions.

Nomenclature

A_c	=	retarding potential analyzer collection area (m^2)
I	=	collector current (A)
$f(V)$	=	ion voltage distribution function
e	=	electron charge (Coulombs)
M	=	ion mass (kg)
n_i	=	plasma density (m^{-3})
V	=	discriminator voltage (V)
Z_i	=	charge state of the collected ion

I. Introduction

THERE is continuing development by NASA of Hall thrusters that can provide high thrust and long life for NASA's deep space missions. In order to extend the development of very high-power Hall thruster specifically to enable cargo

[1] Ph.D. Candidate, University of Pisa, JPL Graduate Research Internship, giulia.becatti@jpl.nasa.gov
[2] JPL Fellow, Electric Propulsion Group, dan.m.goebel@jpl.nasa.gov
[3] JPL Summer Intern, University of South Carolina, cyoke@email.sc.edu
[4] Member of the Technical Staff, Electric Propulsion Group, alejandro.lopez.ortega@jpl.nasa.gov
[5] Principal Engineer, Electric Propulsion Group, ioannis.g.mikellides@jpl.nasa.gov

mission to Mars, NASA has been funding the NextSTEP[1] (Next Space Technologies for Exploration Partnerships) Program. Under the NextSTEP program, Aerojet Rocketdyne (AR) led a team composed of NASA Glenn Research Center (GRC), NASA Jet Propulsion Laboratory (JPL), and the University of Michigan (UM) to advance the development of the XR-100, a 100-kW class Hall Thruster propulsion system[2]. The XR-100 propulsion system consists of UM's X3 Nested Hall Thruster (NHT), JPL's high current hollow cathode, AR's modular Power Processing Unit (PPU), and AR's modular Mass Flow Controller (MFC). The X3 nested-channel Hall thruster[3] operates at discharge power levels from 2 to 200-kW, with discharge voltage between 200-800V. The cathode for this thruster is required to operate at discharge currents of 50 – 350 A with lifetimes in excess of 10 khrs.

In the past 10 years, several LaB_6 hollow cathodes have been developed at JPL for use in high power Hall thrusters[4-6]. The smallest version of this cathode has been operated in xenon from 5 A to 60 A continuously and used extensively in the 6-kW H6 Hall thruster at JPL, UM, and Air Force Research Laboratory. The mid-sized version has operated at 5 to 200 A, and extensively life tested at discharge currents of 25 A for use in the Hermes 12.5 kW Hall thruster[7]. The largest version is intended for use in very high-power Hall thrusters such as the nested-channel X3 Hall thruster[3]. This cathode has been tested at discharge currents of 330 A in the laboratory and up to 250 A in the X3 Hall thruster[8]. The previous version of the cathode was tested at JPL at discharge current of up to 250 A. The newest version of this cathode was designed to reduce orifice plate temperatures to prevent overheating at discharge currents over 300 A, and to utilize injection of auxiliary gas into the near-cathode plasma plume from both the cathode-to-keeper gap and exterior gas injectors to damp oscillations and minimize energetic ion generation at high currents[9]. This "Gen3" cathode has been tested at discharge currents from 25 to 330 A and is predicted to be capable of producing over 350 A of discharge current.

The X3 cathode has been extensively experimentally characterized to evaluate the effect of the design improvements. In particular, the orifice plate temperature has been recorded for the different plate dimensions, and the effect of neutral injection has been verified by measuring the cathode electrical parameters, the plasma oscillations and the energetic ions production in the near plume region. Moreover, the plasma parameters have been measured in different cathode locations. Fast-scanning probes have been used to produce on-axis density, temperature and potential profiles from the upstream end of the insert inside the cathode all the way through the plasma plume exterior to the cathode. Radial scanning probes have been implemented to evaluate the plasma parameters in the radial direction close to the keeper exit plane. An extensive theoretical analysis has been performed, with the application of the decennially developed OrCa2D model[11] to the high current cathode here described. The model simulated the experimentally tested conditions and the insert temperature profiles from the simulations are used in lifetime evaluations based on an insert evaporation life model[12].

This paper is organized as following: Section II presents the cathode description, with a discussion on the improvements in the cathode design that permits high current operation; Section III describes the experimental setup in the JPL cathode facility for the cathode characterization and the plasma diagnostics; Section IV describes the modelling approach for high current cathode; Section V and Section VI present the experimental and the simulation results.

II. X3 Cathode description

A. LaB_6 Characteristics

Lanthanum hexaboride was first developed as an electron emitter by Lafferty[13] in the 1950's and its characteristics extensively described in our previous publications. Lanthanum hexaboride is a crystalline material made by press-sintering LaB_6 powder into rods and then electron-discharge machining the material to the desired shape for an insert into the hollow cathode. Polycrystalline LaB_6 cathodes have a work function of about 2.67 eV depending on the surface stoichiometry[14], and will emit over 10 A/cm^2 at a temperature of 1650 ˚C. The bulk LaB_6 material is the thermionic electron emitter, and there is no chemistry involved in establishing the low work function surface. LaB_6 heated to over 1300 ˚C in reasonable vacuum below 10^{-3} Torr will evaporate any oxide surface layers produced during air exposure and eventually restore the nominal LaB_6 stoichiometry. Therefore, LaB_6 cathodes are insensitive to impurities and air exposures that would normally destroy a BaO dispenser cathode. The life of the LaB_6 cathode is determined primarily by the evaporation rate of the bulk LaB_6 insert material at typical operating temperatures[15-17].

The major reason for using LaB_6 cathodes, as compared to conventional impregnated dispenser cathodes, is the incredible robustness, high current density and long life exhibited by LaB_6 electron emitters[18]. Lanthanum hexaboride cathodes are routinely used in all noble gases from helium to xenon, reactive gases including hydrogen and oxygen, and various other materials including liquid metals such as lithium and bismuth. LaB_6 cathodes have even been successfully used in oxygen and nitrogen plasma discharges at emission current densities exceeding 20 A/cm^2 and vented to water vapor (from cooling lines breaking) and air during operation without damaging the cathode. Lanthanum hexaboride inserts are ideally suited for high current operation in hollow cathodes because they operate at sufficiently high temperatures (>1600 ˚C) to radiate excessive heating from the high density insert plasma generated during high current operation. LaB_6 hollow cathodes have been successfully operated at over 800 A, and the cathode geometry discussed here has operated continuously at discharge currents of up to 330 A. The space heritage of LaB_6 cathodes in Russian and US spacecraft is considerable, and the university and industrial experience in dealing with the higher operating temperatures and materials compatibility issues is extensive.

B. Cathode Design and Upgrades

The LaB_6 hollow cathodes described here for space applications are configured in a geometry similar to conventional space dispenser hollow cathodes[18], which basically consists of an active thermionic insert placed inside a structural cathode tube that is wrapped by a heater, heat shields, and keeper electrode. LaB_6 cathodes of this design have been fabricated with insert outside diameters of 0.63-cm to 2-cm and hollow-cathode lengths from the exit orifice to the base flange from 6 cm to 15 cm for applications in different thrusters that require various cathode sizes[4]. The small LaB_6 hollow cathode with the 0.63-cm-outer-dia. insert was previously described in detail[5] and operated at discharge currents of 10 to 60 A. Likewise, the 1.5-cm diameter insert cathode was designed for operation from 10 to 100 A and tested at discharge currents of up to 200 A[19]. Recently, a miniaturized version of the LaB_6 cathode has been designed to provide discharge currents in the 0.5-4 A range[20], with the sole difference of not including a heater to produce the ignition.

The cathode that is the subject of this paper[21] is the largest of this family of cathodes with a 2-cm outer-dia. insert, a 3.5-cm outer-dia. keeper, and a 15-cm total cathode length. This cathode was originally designed to run from 25 to 350 A and has been tested at steady state discharge currents from 5 A to 330 A, limited to date only by the discharge power supply.

The material in contact with the LaB_6 insert is typically made of graphite because it has a similar coefficient of thermal expansion[22] as LaB_6 and inhibits boron diffusion in to support materials at high temperature. The cathode tube is normally made from a refractory metal such as molybdenum or Mo-Re, with graphite sleeves used to interface with and contact the LaB_6 insert. A schematic representation of the molybdenum-tube configuration for the 2-cm-dia. LaB_6 hollow cathode[21] is shown in Fig. 1. The keeper electrode used to start the discharge is also fabricated from graphite. The heater is a tantalum sheathed heater with high temperature alumina powder insulation[23]. The LaB_6 emitter is configured as a cylindrical insert and is placed inside the hollow molybdenum tube. The LaB_6 insert is held in place with a tungsten spring and refractory metal or graphite "pusher tube" placed inside the cathode tube. In the latest versions of the cathode8, a radiation shield consisting of multiple layers of moly disks has been inserted between the pusher and the insert to reduce the heat loss from the insert axially upstream. This improves the thermal efficiency of the cathode and reduces the axial temperature gradient in the insert. The cathode tube is sufficiently long and thin to minimize conduction of heat from the insert to the base plate.

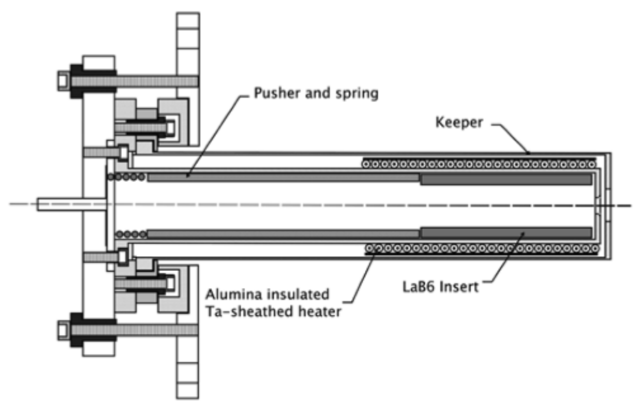

Figure 1 Schematic of the 2-cm-dia. LaB6 hollow cathode.

The insert in this larger cathode case has an outer diameter of about 2 cm, an inside diameter of 1.3 cm and a length of 5 cm, which provides 20 cm^2 of emission area exposed to the plasma inside the hollow cathode insert. If the emission is uniform along the length of the insert, at an insert temperature of 1700 ˚C this cathode can emit nearly 20 A/cm^2 and produce total current of over 350 A. A photograph of the cathode as configured to use in the Hall thruster is shown in Figure 3.

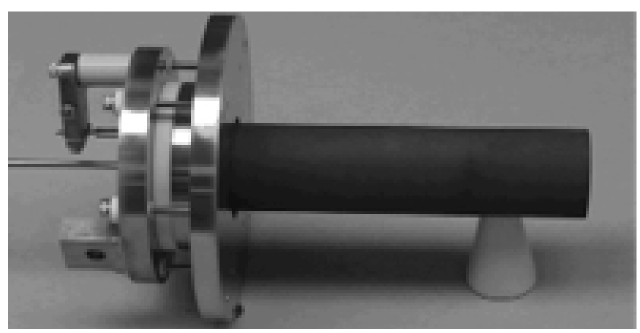

Figure 3 The laboratory-model 2-cm-dia. LaB6 hollow cathode.

A major issue with the original configuration of this cathode was excessive orifice plate temperatures at discharge currents over 150 A. This problem was mitigated by increasing the outer diameter of the cathode orifice plate from 2.2 cm to 2.9 cm and finally 3.2cm, which is slightly larger than the diameter of the heater and heat shield. This significantly increases the radiation area and reduces the plate temperature. Figure 4 shows the original design (a) with the orifice being the same diameter as the cathode tube, the 2nd generation version (b), and the 3rd generation version (c) with the enlarged diameter orifice plate. The only issue in fabrication of this geometry was that the heater has to be wound and installed on the cathode tube before the tungsten orifice plate is e-beam welded onto the cathode tube. The effectiveness of this solution has been experimentally investigated by measuring the orifice plate temperature during cathode steady discharge current operation. The results of this investigation are presented in Section V.

Figure 4 Original cathode orifice plate (a) and a versions (b) and (c) with a larger diameter orifice plates

Previous investigation on the first generation of the 2cm-out-dia cathode highlighted the fundamental role of additional gas injection to suppress the instabilities as the cathode current is increased[9] and to lower the discharge voltage in the test facility. Additionally, the gas injection proved to reduce the production of energetic ions in the cathode plume, which would increase the keeper erosion and limit the lifetime[25-36].

The cathode and gas injector assembly used in the tests in the X3 Hall thruster is shown in Figure 5. An additional gas injection path between the cathode tube and keeper tube was also introduced into this updated cathode design. This path injects neutral gas directly into the cathode plume through the keeper orifice without significantly affecting the pressure inside the cathode insert region. The flow through the cathode and the internal pressure is optimized to produce a relatively flat density profile and plasma contact with the entire length of the insert for uniform thermionic emission, while the gas injectors reduce the energetic ions produced outside the cathode insert region.

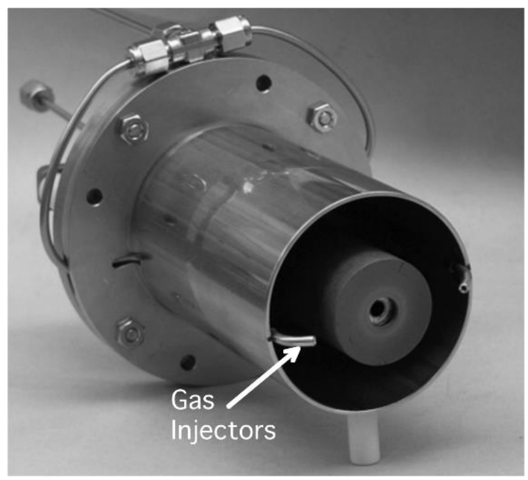

Figure 5 Lanthanum hexaboride hollow cathode assembly with cathode-plume gas injectors.

III.Experimental Setup

The cathode was operated in one of the JPL cathode test facilities[25] at discharge currents up to 330 A. The cathode installed in the test facility is shown in Figure 6. The facility has a 1-m-dia. by 2.2-m-long vacuum system with 1250 l/sec xenon pumping speed from two cryo-pumps. A solenoid coil is positioned around the keeper electrode to provide an adjustable axial magnetic field at the cathode exit. The anode consists of a water-cooled cylinder of 10-cm area to handle the high-power discharge. This test configuration produces discharge voltages in the 15 to 30 V range, depending on the current and gas flow rate.

A series of plasma diagnostics has been employed for the cathode plasma characterization both of the internal and external regions.

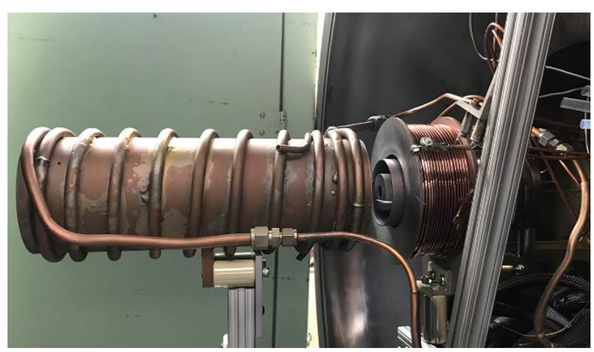

Figure 6 High power test facility setup with gas injectors.

First, the X3 cathode has been mounted on the fast scanning Langmuir probe setup developed at JPL for internal and external cathode plasma parameters measurements[37].

The internal fast scanning Langmuir probe is used to produce axial profiles of the plasma density, electron temperature, and plasma potential inside the hollow cathode. The Langmuir probe has a 0.1-mm-diam, 1-mm-long tungsten electrode tip supported by a 0.78-mm-diam alumina tube connected to a pneumatic drive mechanism outside the vacuum chamber. The probe moves at up to1 m/s and can scan up to 10cm in and out in less than 0.1 s. The probe is nominally biased to ion saturation during the scan, with periodic 2 ms sweeps of the probe voltage to obtain the electron temperature and plasma potential points. This technique avoids melting of the probe in the high-density plasma inside the insert region. A similar pneumatic mechanism is used to scan the external Langmuir probe along the cathode centerline in the plume region. The "anode" probe can scan the whole anode length region up to the keeper entrance. The diameter of the ceramic tubing is stepped down from 3 mm at the pneumatic driver to 0.78 mm diameter in order to minimize perturbation to the plasma in the anode region. The exposed electrode is a 0.25-mm-diameter tungsten wire with a length of 1 mm in order to collect sufficient current away from the keeper region to accurately determine the plasma parameters.

Second, a dedicated radial scanning mechanism has been implemented to evaluate the plasma parameters variation along the radial direction close to the keeeper exit. Standard, high-vacuum electrical motors have been used for the radial probe scan system. The selected motor is used to move a linear stage at a speed up to 20 cm/s. The system is designed to minimize electrical interference with the probe measurement. An emissive probe and a Langmuir probe have been mounted on the radial scanning system to obtain the radial profiles of plasma voltage and plasma density. The emissive probe has a 0.25mm dia. tungsten filament tip, insulated with a 0.7mm diam. alumina tube connected with the linear stage. The emissive probe is operated by applying a constant current, to increase the probe tip temperature and directly measuring the plasma potential[38]. In order to reduce the emissive probe evaporation and therefore increase its life, the applied constant current is provided only during the probe scan. The Langmuir probe, shown in Figure 7a, has a 0.25mm diameter tungsten exposed tip, constantly biased to ion saturation. The scanning system, has been designed to collect the plasma parameters between the radial anode entrance and the cathode axis.

The final diagnostic system employed to analyze the X3 cathode plasma is a miniaturized retarding potential analyzer (RPA). The retarding potential analizer is a useful plasma diagnostic to measure the ion energy distribution, and it has been used many times at JPL[8,9,25]. The RPA implemented in the X3 "Gen. 3" cathode test has been specifically developed to measure the production of energetic ions along the keeper face. The RPA is 5 mm in diameter and 3mm thick, and it has been mounted on the radial scanning system described above. With this configuration, the probe can be scan in the radial direction close to the keeper face and measure the energetic ions directly impacting the keeper, as shown in Figure 7. The first grid of the RPA is biased at a negative potential (-25V) to repel the electrons. The second grid the discriminator grid, is swept with the ramp voltage applied at a fixed frequency and amplitude. The third electrode is the collector.

Using the radial scanning system, the RPA is inserted in the cathode plume at the desired position, the measurement is acquired, and then the probe is retracted back to the rest position in less then 2s to avoid overheating of the probe.

a) b)

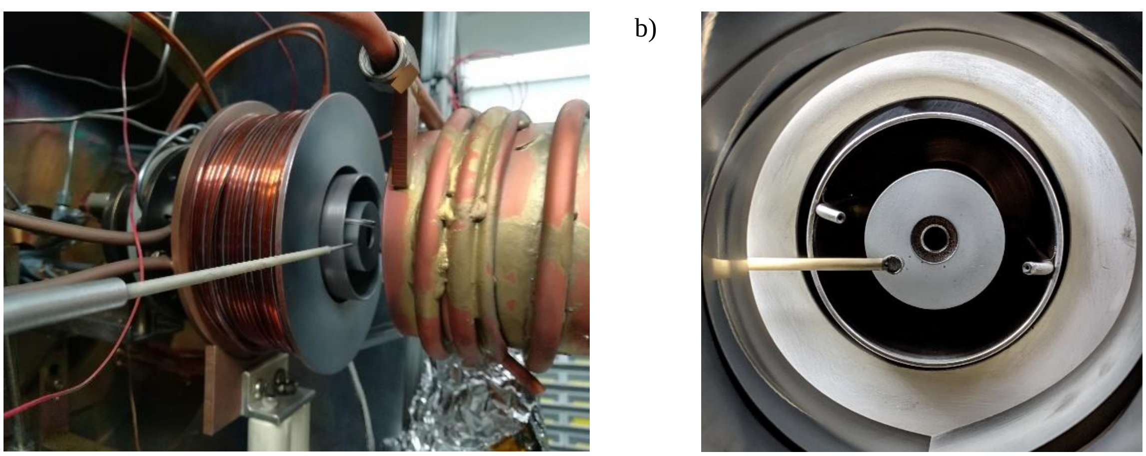

Figure 7 a) Radial scanning probe system view, b) RPA probe measurement position.

IV.Cathode modelling

The physics models and numerical methods in OrCa2D have been described in detail in [26-32] and will only be described briefly here. OrCa2D solves conservation laws for the three species present in a partially ionized gas: electrons, xenon ions, and xenon neutrals. Inside the cathode, the Navier-Stokes equations for neutral xenon are solved using an implicit backward Euler scheme, which includes the viscous terms. It has been shown that the flow of neutrals transitions from a low to a high Knudsen number downstream of the cathode orifice. Thus, a fluid approximation is not applicable in the cathode plume. Free molecular flow, in which neutrals move in straight paths, is assumed downstream of an axial location, typically chosen to be in the cathode orifice where the Knudsen number approaches unity. Mass and momentum continuity are preserved across the transition boundary. The Euler equations for mass and momentum of charged ions are solved accounting for the effects of ionization, charge exchange and electron-ion collisions. Separate energy equations are used to compute the temperature of ions and neutrals. Inside the cathode tube, the temperatures of both species are very similar due to the dominance of ion-neutral collisions and the assumption of the ion temperature being equal to the neutral temperature has been used in the past. However, it was shown in [32] that collisionless heating of ions due to ion-acoustic turbulence (IAT) drives their temperature in the cathode plume, and therefore a separate equation for ions and neutrals is needed. Finally, the plasma parameters for electrons are determined from the solution of the electron energy equation and the combination of the current conservation equation with the vector form of Ohm's law that accounts for the presence of the magnetic field induced by the plasma currents in the cathode[32]. The resistivity in Ohm's law is determined as a function of the classical collision frequencies (i.e., electron-ion and electron-neutral) and the anomalous collision frequency that models the effect of the IAT on the electron transport.

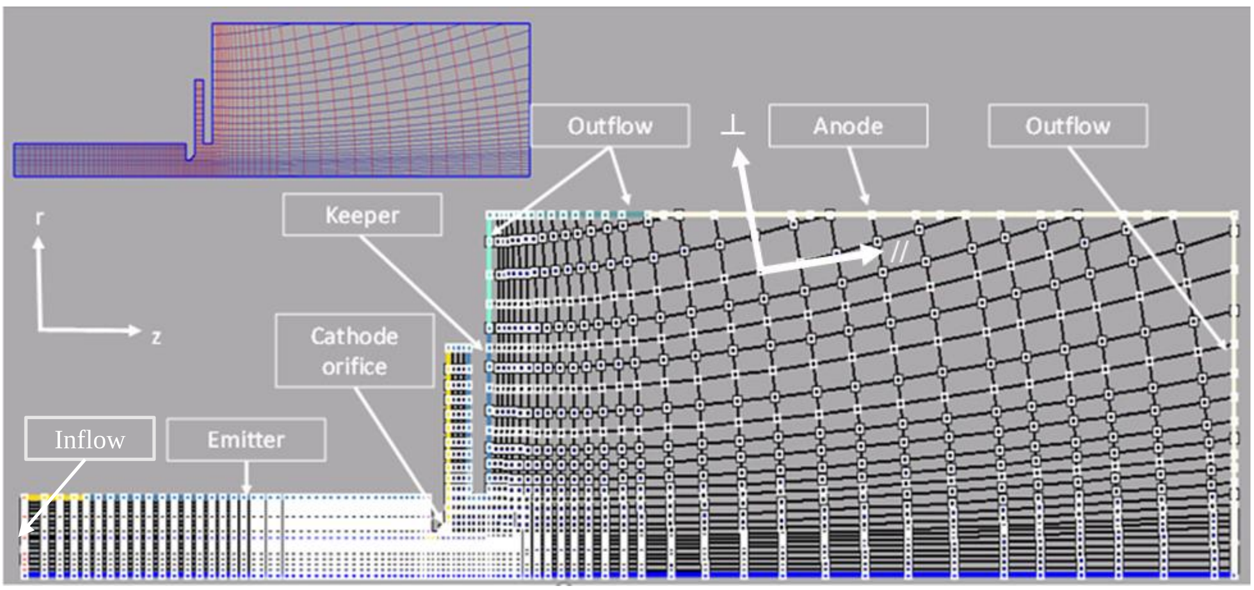

Figure 8 Example of OrCa2D computational domain and mesh pointing to the different boundary conditions. The mesh in the cathode interior is rectilinear and a magnetic-field-aligned mesh (MFAM) is used for the plume.

The computational domain (Figure 8) comprises the interior of the cathode tube and a considerable section (in the order of tens of centimeters) of the plume, which includes the collecting surface of the anode. The computational domain is designed in a way such that it can replicate the exact conditions at which a cathode test was run in the laboratory. Since a magnetic-field-aligned mesh (MFAM)[33-34] simplifies the solution of Ohm's law, the computational mesh can be made aligned to an applied external magnetic field if one existed in the laboratory test.

Conductor boundary conditions are applied at the emitter, orifice, keeper, and anode. These conditions assume an infinitesimally small sheath that can be modeled as one-dimensional. In addition, the total electron current from the emitter is the difference between the emitted and absorbed current. The emitted current is determined by the Richardson-Dursham[35] emission equation. The emitter temperature is specified as an input based on available laboratory measurements.

V. Experimental Results

C. LaB₆ Cathode Discharge Performance

After installation in the test facility, the system was pumped down into the 10^{-6} torr range and the cathode heater turned on for 16 minutes. The cathode discharge was then started by initiating the xenon gas flow through the cathode, applying 150 V to the keeper electrode and turning on the anode power supply. The keeper current was regulated to 2 A, and the keeper voltage fell to a value typically in the 5 to 10 V range depending on the gas flow rate. Once the anode discharge current exceeded 10 A, the heater and keeper power supplies were turned off and the keeper allowed to float. The cathode was normally run at 25 A for a minute or two until the discharge voltage stabilized, and then it could be turned up to full current in less than a minute.

Figure 9a shows the cathode discharge current versus discharge voltage characteristics for various gas flows through the insert and external to the cathode orifice plate. By providing 20 sccm additional gas injection, the cathode can easily run up to 330A with discharge voltage lower than 30V. The discharge current versus voltage characteristics for this updated cathode are largely unchanged from the previously published version[24].

Figure 9b shows the keeper voltage peak-to-peak at the cathode nominal operating conditions. The keeper voltage peak-to-peak is considered an indication of the transition to plume mode[36,39,40], when the oscillations in the plasma start to increase, and it is associated with an sudden increase of the keeper wear with a limitation in the cathode life. As seen in Figure 9b, the P2P keeper voltage increases as the discharge current increases, and it decreases at higher cathode flow rate or higher external gas injection. Increasing the cathode injection is found to be particularly efficient in damping the keeper voltage oscillations, ensuring the cathode to operate in the stable spot mode.

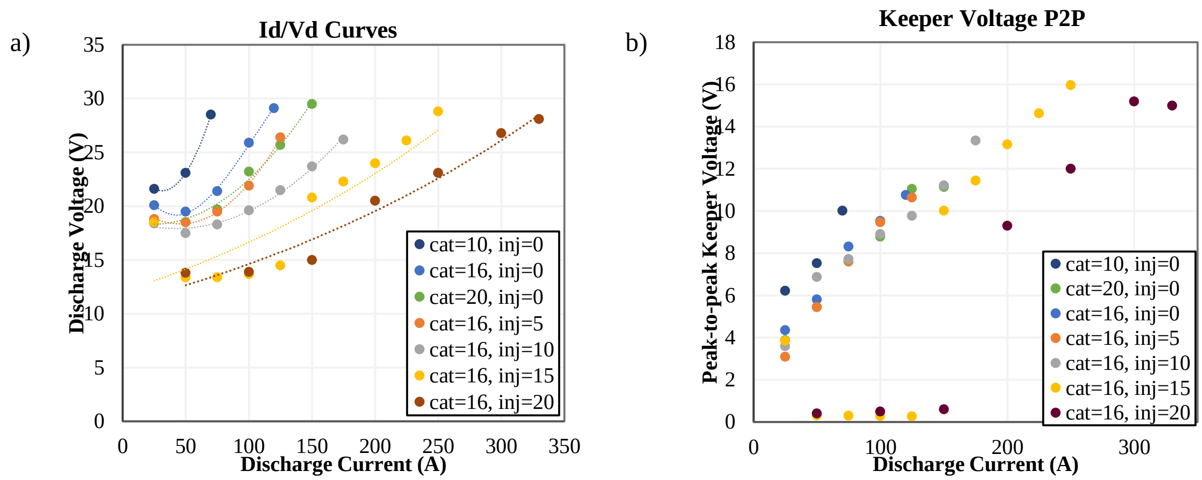

Figure 9 X3 cathode electrical characteristics: a) discharge current/discharge voltage curve, b) discharge current/keeper voltage peak-to-peak curve.

D. Orifice Plate temperature

Temperature measurements of the cathode orifice plate are made using a DFP 2000 Disappearing Filament Optical Pyrometer calibrated by a tungsten filament reference in the vacuum system. A comparison of the measured temperature of the filament to that derived from simple radiation theory was used to obtain a calibration curve to correct the readings of the orifice plate temperature through the vacuum system window. The temperature of the orifice plate as a function of discharge current for the three different cathode-orifice-plate configurations is shown in Figure 10. The original design produced orifice plate temperature over 2200 ˚C at 250 A, while the "Gen. 2" diameter orifice plate design maintained

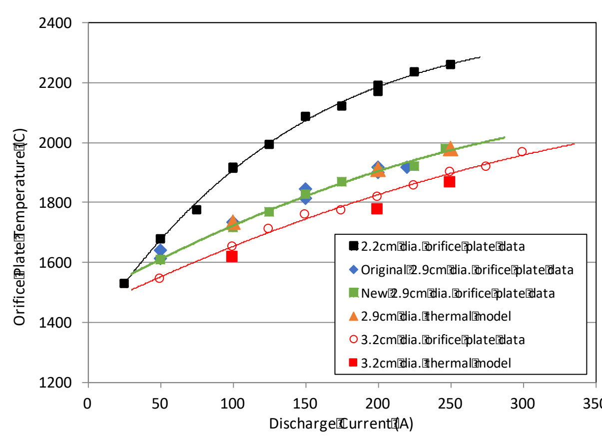

Figure 10 Orifice plate temperature for three orifice plate diameters at discharge currents of up to 300 A.

the orifice plate well below 2000 ˚C at about 225 A. Since the orifice plate temperature was the major factor limiting the discharge current, this improved design permitted reliable operation of the cathode at up to 250 A of discharge current. However, this will still result in excessive temperatures for operation at the planned 350 A for the highest power levels of the X3 thruster. Therefore, X3 "Gen. 3" cathode was provided with a larger diameter orifice plate to provide this capability. The new orifice plate dimension proved to maintain the temperature below 2100 °C at 330A.

E. Internal and External Plasma Parameters

The ability to experimentally measure the cathode plasma parameters at the operative conditions is of vital importance for the development of an engineering model intended to proceed in the development of a flight model. In fact, the cathode lifetime in terms of the emitter evaporation and keeper electrode wearing can be assessed with the knowledge of the plasma parameters in the interior and exterior region of the cathode. Moreover, the results of experimental plasma measurements can be used to benchmark the cathode plasma model and predict the main lifetime limiting factors.

The importance in hollow cathodes of the axial plasma density is clearly stated in past publications[6,12,37]. An axially uniform internal plasma density results in a more uniform insert temperature profile, and therefore a uniform evaporation rate of the LaB6[41,42]. It should also be considered that space charge can limit the thermionic emission current if the plasma density becomes too low toward the upstream end of the insert, limiting the effective emission area and how much current the insert can emit into the plasma.

Figure 11 shows the plasma density profiles as a function of position along the cathode axis from the upstream internal insert region up to the external far plume for various discharge currents up to 200 A at 16 sccm (Figure 11a) and 20 sccm (Figure 11b) cathode flow conditions.

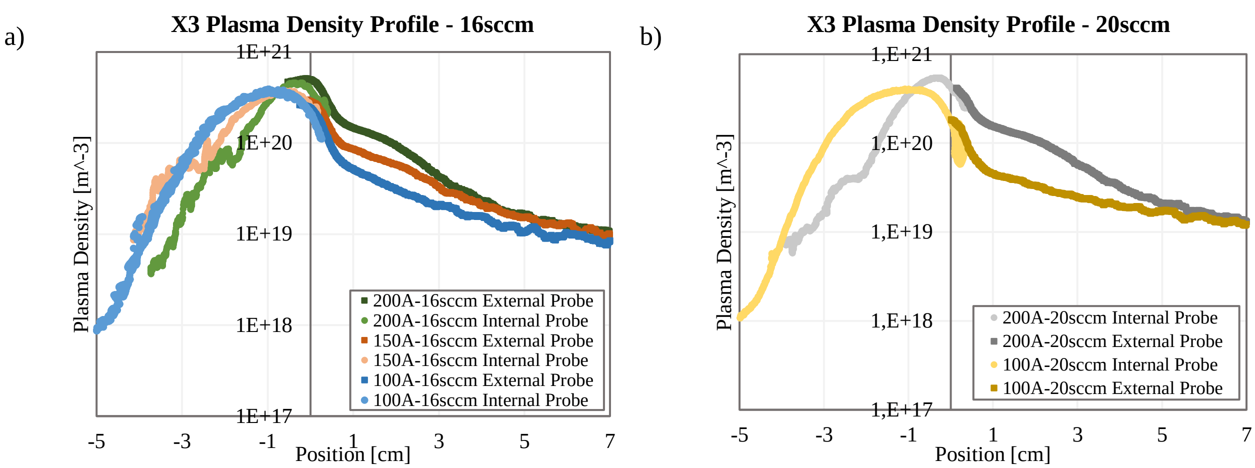

Figure 11 X3 cathode axial plasma density profiles a) at 16sccm, b) at 20sccm.

The electron temperature in the insert region is about 2.5±0.5 eV and the plasma potential inside the insert varied from about 14V down 8V as the discharge current increased. In the plume region the electron temperature values are between 2 and 5 eV, and the plasma potential on axis varies in the 10-20 V range.

The internal plasma density shows a peak in the downstream insert region, and, as observed previously in hollow cathodes[20], the plasma density shifts downstream toward the orifice plate at higher discharge currents and higher flow rates. The plasma contact area with the 5-cm long insert in the high current cathode may be limited at currents below 100 A. Moreover, the large plasma density gradient along the insert region would likely affect the insert temperature gradient[41]. To this end, a set of heat shields were installed inside the cathode just upstream of the insert to minimize radiation losses from the insert to the cathode tube and back flange.

The external plasma density profile shows a decreasing behavior typical of the cathode plume region, more accentuated at the low currents. Interestingly, the external and internal probes measurement in the cathode-to-keeper region produced the same plasma parameters. This is an indication of the low perturbation caused by the probes inserted from both directions and scanning along the whole discharge path.

Figure 12 shows the radial plasma potential measured with the scanning emissive probe at about 6 mm distance with the keeper face. The results show the typical behavior in the hollow cathode plume[36], with the minimum in the potential found along the cathode axis and a gradual increase along the keeper face.

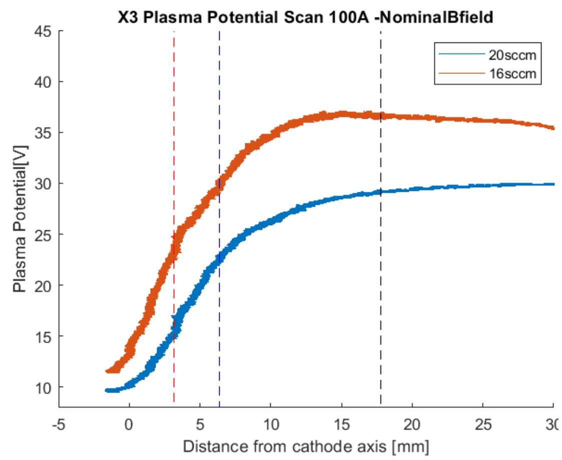

Figure 12 X3 radial plasma potential profiles.

F. Energetic Ions Production

As observed with the previous version of this cathode, the production of high-energy ions in the near-cathode plume of hollow cathodes increases significantly with discharge current. These ions sputter-erode the cathode keeper and cathode orifice plate, which strongly impacts the cathode life.

The energetic ions are produced by either plasma potential fluctuations from ionization instabilities in the thruster plume[36], or by turbulent ion acoustic waves or drift waves[10] also in the near cathode plume. The miniaturized three-grid RPA was used to measure the ion energy distribution at discharge currents up to 3300 A. The ion energy distribution is proportional to the first derivative of the current-voltage characteristic obtained from the RPA, and is related to the ion voltage distribution function f(V) by:

$$\frac{dI}{dV} = -\frac{{Z_i}^2\, e^2\, n_i\, A_c}{M} f(V)$$

where Z_i is the charge-state of the ion, e is the electron charge, n_i is the ion density, A_c is the probe collection area, and M is the mass of the xenon ion. Due to the noise in the collected current signal, current-voltage data from the RPA is fit to a 17th-order polynomial and the derivative of that polynomial fit used to determine the ion energy distribution.

Figure 13a shows the ion energy distribution at up to 330A with the cathode operating at 16 sccm of flow injection and 20 sccm of additional external injection. As observed in previous publication, the energy of the ions increases with discharge current, reaching more than 60V at 330A. The injection of external flow is found to be effective in reducing the production of energetic ions. In fact, as see in Figure 13b, ions with energy up to 60V are found when the cathode is operated at 16 sccm without additional flow. The energy of the ions is then less than 20V when the external gas is employed.

a)

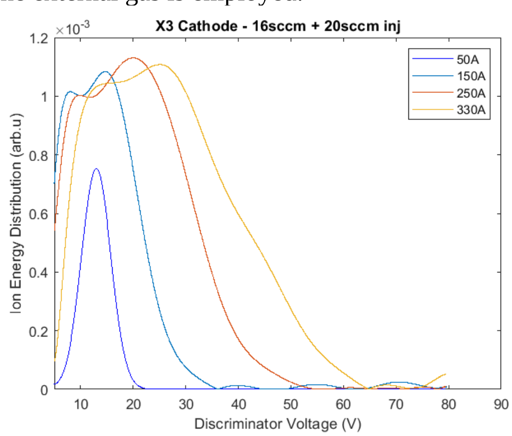

b)

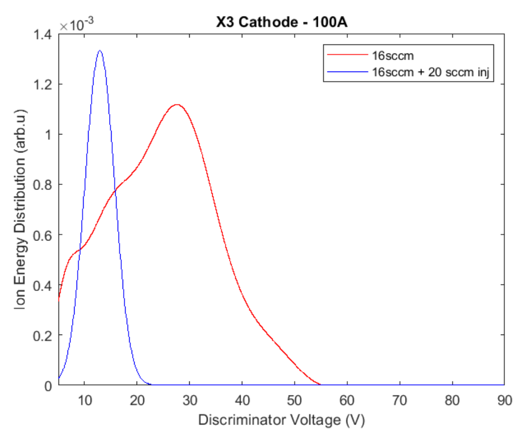

Figure 13 Ion energy distribution at a) discharge current up to 330A and b) at 100A with and without external injection.

VI.OrCa2D Model Results

OrCa2D has successfully been used to model the plume margin as a function of the flow rate of the LaB_6 cathode for HERMeS operating at the nominal condition of 25 A[43-44] . In the near future, we plan to extend that investigation to the X3 cathode and include operation at multiple discharge currents, mass flow rates (with and without external injection) and magnetic fields. Before this can be accomplished, we must first validate the steady-state numerical solutions with laboratory measurements at a few key operating conditions. This is the topic of this section.

Figure 14 depicts the ~~axial~~ comparison between the measured and computed plasma density along the cathode centerline for three operating conditions in which the mass flow rate is 20 sccm and the discharge current is 25, 100 and 200 A. We considered the presence of the applied magnetic field only for the 200-A condition as measurements at this condition could not be obtained in the absence of a magnetic field. We observe excellent agreement with the measurements. The computed plasma density is found typically to be within the uncertainty (quantified to be approximately a factor of two) of the measurement for all the operating conditions. A similar level of agreement has been found for other plasma properties, such as the internal electron temperature and plasma potential (within 1 eV of the measurement).

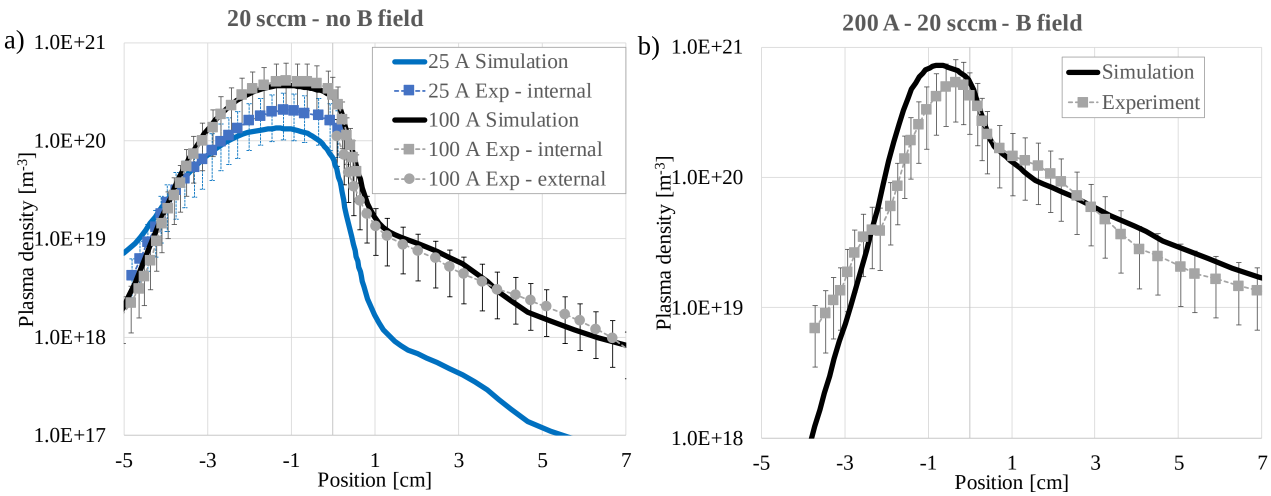

Figure 14 Plasma density comparison along cathode centerline between numerical simulations and experimental measurements for operating conditions at 20 sccm and 25, 100 A (a) and 200 A (b). 200-A condition with applied magnetic field.

We also made modifications to OrCa2D to allow injection of neutral gas at locations different than the inflow boundary (red boundary in Fig. Figure 4). Figure 15 shows an example in which neutral gas has been injected in an axisymmetric manner in the gap between the orifice plate and the keeper electrode. The operating condition is 20 sccm – 100 A and 50 sccm are injected in the gap. We observe that the neutral injection increases the neutral and plasma density immediately downstream of the keeper exit. It was shown in [32] that the ion-neutral collision frequency, which is proportional to the neutral density, acts as a damping term in the growth rate of the IAT that develops in the cathode plume (which in turn leads to the formation of a high-energy tail in the distribution function of the ions). With this addition, OrCa2D can directly be used to quantify the effectiveness of neutral injection in preventing the excitement of IAT and the formation of high-energy ions in the cathode plume.

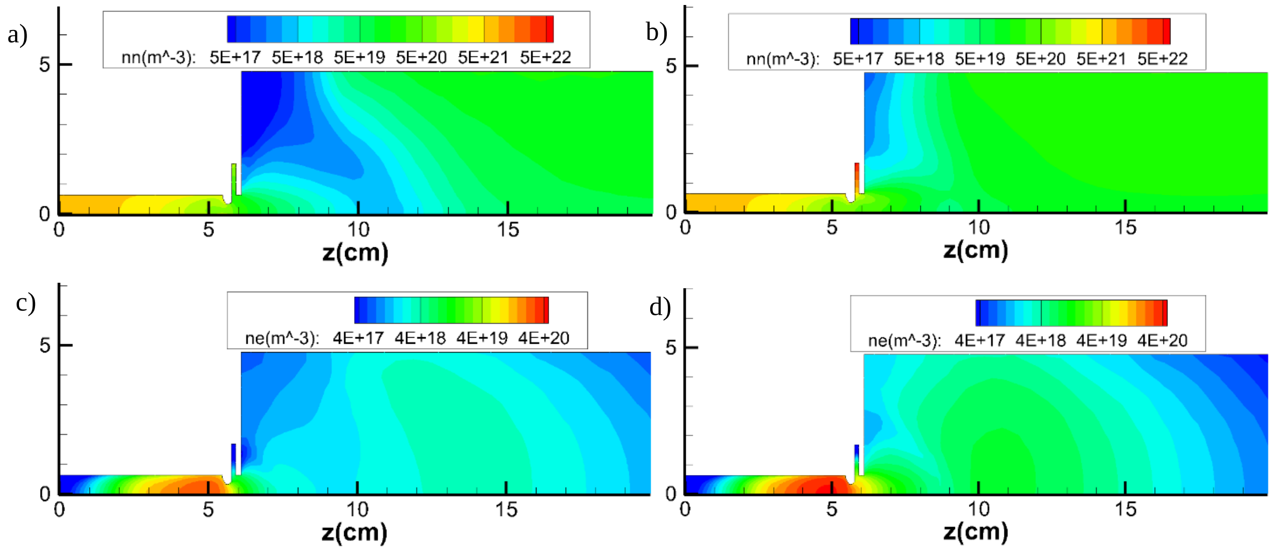

Figure 15 Density contours of neutral density (top) and plasma density (bottom) for the X3 cathode operating at 20 sccm - 100 A. Left: without additional neutral injection, right: additional 50 sccm mass flow rate of xenon at the gap between orifice and keeper

VII.Conclusions

The high current X3 LaB6 hollow cathode, developed at JPL during the past 5 years, has been successfully tested in the X3 thruster at discharge current up to 250A and in the stand-alone tests at up to 330A. The cathode design has been upgraded and can now provide discharge currents ranging from 10 to 350 A. This cathode design features a robust molybdenum cathode tube, a tungsten cathode orifice plate and a graphite keeper. The tantalum sheathed heater technology that uses Al_2O_3-powder insulation has proven to be very reliable in heating these higher temperature cathodes to ignition. The high-current hollow cathode assembly includes internal gas injectors between the keeper and the cathode tube to reduce the energetic ion production in the near-cathode region that can limit the life of the keeper electrode at the very high discharge currents that this cathode has demonstrated.

The X3 cathode has been experimentally tested to measure the plasma parameters along the cathode axis with the fast-scanning Langmuir probe at discharge current up to 200A, and along the radial direction close to the keeper exit plane with the emissive probe and the miniaturized retarding potential analyzer at discharge current up to 300A.

The 2-D axisymmetric code OrCa2D was employed to simulate the plasma conditions of the X3 cathode. We made modifications to the code to enable injection of neutral atoms at locations different from the cathode tube. We compared the code results with measured plasma parameters both in the cathode interior and in plume region, at a range of operating conditions (25-200 A) spanning most of the operating envelope of the cathode. We found that simulation results and measurements are separated by less than the experimental uncertainty in most locations and operating conditions. We also showed an example of the effect of neutral injection in the gap between the orifice plate and the keeper. As a result, the neutral density increases immediately downstream of the plume. Qualitatively, this leads to lower growth rates of the ion-acoustic turbulence which has been argued to be the mechanism behind the formation of high-energy ions in the cathode plume.

Acknowledgement

The research described in this paper was carried out by the Jet Propulsion Laboratory, California Institute of Technology, under a contract with the National Aeronautics and Space Administration.

References

[1]Shark, Sarah W., et al. "High Power Demonstration of a 100 kW Nested Hall Thruster System." AIAA Propulsion and Energy 2019 Forum. 2019.

[2]Jackson, Jerry, et al. "100 kW Nested Hall Thruster System Development." (2017).

[3]S.J. Hall, B.A. Jorns, A.D. Gallimore, H. Kamhawi, T.W. Haag, J.A. Mackey, J.H. Gilland, P.Y. Peterson, and M.J. Baird, "High-Power Performance of a 100-kW Class Nested Hall Thruster", IEPC-2017-228, 35th International Electric Propulsion Conference, Electric Rocket Propulsion Society, Atlanta, GA, 2017.

[4]Goebel, Dan M., Ron M. Watkins, and Kristina K. Jameson. "LaB6 hollow cathodes for ion and Hall thrusters." Journal of Propulsion and Power 23.3 (2007): 552-558.

[5]Goebel, Dan M., and Ronald M. Watkins. "Compact lanthanum hexaboride hollow cathode." Review of Scientific Instruments81.8 (2010): 083504.

[6]Goebel, Dan M., and Emily Chu. "High-current lanthanum hexaboride hollow cathode for high-power hall thrusters." Journal of Propulsion and Power 30.1 (2013): 35-40.

[7]Hofer, Richard R., et al. "The 12.5 kW Hall effect rocket with magnetic shielding (HERMeS) for the asteroid redirect robotic mission." 52nd AIAA/SAE/ASEE Joint Propulsion Conference. 2016.

[8]Goebel, D. M., Becatti, G., Reilly, S., Tilley, K., and Hall, S. J., “High Current Lanthanum Hexaboride Hollow Cathode for 20-200 kW Hall Thrusters,” IEPC-2017-303, 35th International Electric Propulsion Conference, Electric Rocket Propulsion Society, Atlanta, GA, 2017.

[9]Chu, E., Goebel, D. M., and Wirz, R. E., “Reduction of Energetic Ion Production in Hollow Cathodes by External Gas Injection,” Journal of Propulsion and Power, Vol. 29, No. 5, 2013, pp. 1155–1163. doi:10.2514/1.B34799

[10]B.A. Jorns, I.G. Mikellides, D.M. Goebel, “Ion Acoustic Turbulence in a 100-A LaB6 Hollow Cathode”, Physical Review E, 90, 063106 (2014).

[11]I.G. Mikellades, I.Katz, D.M.Goebel, and K.K. Jameson “Hollow Cathode Theory and Modeling: II. A two-dimensional model of the emitter region”, J. App. Phys., 98(10), 113303 (2005).

[12]G. Becatti, D.M. Goebel, J.E. Polk and P. Guerrero, “Life Evaluation of a Lanthanum Hexaboride Hollow Cathode for High-Power Hall Thrusters”, J. Propulsion and Power, Jan. 2, 2018, DOI: 10.2514/1B36659.

[13]J.M. Lafferty, “Boride cathodes”, J. Appl. Phys., 22, 1951, pp. 299-309.

[14]E.K Storms and B. Mueller, “A study of surface stoichiometry and thermionic emission using LaB6, J. Appl. Phys., 50, 1979, pp. 3691-3698.

[15]E.K. Storms and B. Mueller, “Phase relationship, vaporization and thermodynamic properties of the lanthanum-boron system”, J.Chem. Phys. 82, 1978, pp.51-59.

[16]D. Jacobson and E.K. Storms, “Work function measurement of lanthanum-boron compounds”, IEEE Trans. Plasma Sci., 6, 1978, pp. 191-199.

[17] J. Pelletier and C. Pomot, “Work function of sintered lanthanum hexaboride”, Appl. Phys. Lett., 34, 1979, pp.249-251.

[18]D.M. Goebel and I. Katz, Fundamentals of Electric Propulsion; Ion and Hall Thrusters, J. Wiley and Sons, NJ, 2008.

[19]E. Chu and D.M. Goebel, “High Current Lanthanum Hexaboride Hollow Cathode for 10 to 50 kW Hall Thrusters, IEEE Trans. Plasma Sci., 20, No. 9, 2133-2144 (2012).

[20]R. Conversano et al., “Overview of the Ascendant Sub-kW Transcelestial Electric Propulsion System (ASTRAEUS)”, 36th International Electric Propulsion Conference, IEPC-2019-282

[21]D.M. Goebel and E. Chu, “High Current Lanthanum Hexaboride Hollow Cathode for High Power Hall Thrusters”, J. Propulsion and Power, Vol.30, No. 1, pp 35-40, (2014), doi: 10.2514/1.B34870

[22]C.H. Chen, et al., “Structural refinement and thermal expansion of hexaborides”, Journal of Alloys and Compounds, 366, L6-L8 (2004).

[23]Catalog item from Idaho Labs, Idaho Falls, Idaho.

[24]D.M. Goebel, G. Becatti , S. Reilly , K. Tilley, and S.J. Hall, “High Current Lanthanum Hexaboride Hollow Cathode for 20-200 kW Hall Thrusters”, IEPC-2017-303, 35th International Electric Propulsion Conference, Atlanta, Georgia, October 8-12, 2017.

[25]D.M. Goebel, K. Jameson , R. Watkins, I. Katz, “Hollow Cathode and Keeper-Region Plasma Measurements Using Ultra-Fast Miniature Scanning Probes”, AIAA-2004-3430, 40th AIAA Joint Propulsion Conference, Fort Lauderdale, FL, July 11-14, 2004.

[26]Mikellides, I. G., Katz, I., Goebel, D. M., Jameson, K. K. and Polk, J. E., “Wear Mechanisms in Electron Sources for Ion Propulsion II: Discharge Hollow Cathodes”, Journal of Propulsion of Power, Vol. 24, No 4, 2008, 866-879, doi: 10.2514/1.33462

[27]Mikellides, I. G., Katz, I., D. Goebel, D. M., and Polk, J. E., “Hollow Cathode Theory and Experiment II: A Two-dimensional Theoretical Model of the Emitter Region”, Journal of Applied Physics, Vol. 98, No. 11, 2005, 113303, doi: 10.1063/1.2135409

[28]Mikellides, I. G, Katz, I., Jameson, K. K., and Goebel, D. M., “Numercial Simulations of a Hall Thruster Hollow Cathode Plasma”, IEPC-2015-018, in proceedings of the 30th International Electric Propulsion Conference, Florence, Italy, September 2007.

[29]Mikellides, I. G., Katz, I., Goebel, D. M., Polk, J. E., and Jameson, K. K., “Evidence of Non-classical Plasma Transport in Hollow Cathodes for Electric Propulsion”, Journal of Applied Physics, Vol. 101, No. 6, 2007, 063301, doi: 10.1063/1.2710763

[30]Mikellides, I. G. and Katz, I., “Wear Mechanisms in Electron Sources for Ion Propulsion I: Neutralizer Hollow Cathode”, Journal of Propulsion and Power, Vol. 24, No. 4, 2008, 855-865, doi: 10.2514/1.33461

[31]Mikellides, I. G., Goebel, D. M., Jorns, B. A., Polk, J. E., and Guerrero, P., “Numerical Simulations of the Partially-ionized Gas in a 100-A LaB6 Hollow Cathode”, IEEE Transactions on Plasma Science, Special Issue on Plasma Propulsion, Vol. 43, No. 1, 2015, pp. 173-184, doi: 10.1109/TPS.2014.2320876

[32]Lopez Ortega, A., Jorns, B. A., and Mikellides, I. G., “Hollow Cathode Simulations with a First-Principles Model of Ion-Acoustic Anomalous Resistivity”, Journal of Propulsion and Power, Vol. 34, No. 4, 2018

[33]Marchand, R. and Dumberry, M., “CARRE: a Quasi-orthogonal Mesh Generator for 2D edge Plasma Modelling”, Computer Physics Communications, Vol. 96, 1996, pp. 232-246, doi: 10.1016/0010-4655(96)00052-5

[34]Lin, Z., Hahm, T. S., Lee, W. W., Tang, W. M., and White, R. B., “Turbulent Transport Reduction by Zonal Flows: Massively Parallel Simulations,” Science, Vol. 281, 1998, pp. 1835-1837, doi: 10.1126/science.281.5384.1835

[35]Dusham, S., “Electron Emission from Metals as a Function of Temperature”, Physical Review, Vol. 21, No. 6, 1923, 623-636, doi: 10.1103/PhysRev.23.153

[36]D.M. Goebel, D.M. Goebel, K. Jameson, I. Katz and I. Mikellides, "Potential Fluctuations and Energetic Ion Production in Hollow Cathode Discharges", Physics of Plasmas, 14, 103508 (2007).

[37]Goebel, Dan M., et al. "Hollow cathode theory and experiment. I. Plasma characterization using fast miniature scanning probes." Journal of Applied Physics 98.11 (2005): 113302.

[38]Sheehan, J. P., et al. "Recommended practice for use of emissive probes in electric propulsion testing." Journal of Propulsion and Power 33.3 (2016): 614-637.

[39]Sengupta, Anita, et al. "An Overview of the Results from the 30,000 Hr Life Test of Deep Space 1 Flight Spare Ion Engine." 40th AIAA/ASME/SAE/ASEE Joint Propulsion Conference and Exhibit. 2004.

[40]Brophy, John, And Charles Garner. "Tests of high current hollow cathodes for ion engines." 24th Joint Propulsion Conference. 1988.

[41]Polk, J. E., D. M. Goebel, and P. Guerrero. "Thermal Characteristics of Lanthanum Hexaboride Hollow Cathodes." 34th International Electric Propulsion Conference, IEPC-2015-044, Kobe, Japan. 2015.

[42]Guerrero, P., I. G. Mikellides, and J. E. Polk. "Hollow cathode thermal modelling and self-consistent solutions. Work function evaluation for a LaB6 cathode." 54th AIAA/SAE/ASEE Joint Propulsion Conference, 2018.

[43]Mikellides, I. G., Guerrero, P., Lopez Ortega, A., and Polk, J. E., "Spot-to-Plume Mode Transition Investigations in the HERMeS Hollow Cathode Discharge Using 2-D Axisymmetric Plasma Simulations", AIAA 2018-4722, 2018 Joint Propulsion Conference, Cincinnati, OH, July 2018

[44]Mikellides, I. G., Lopez Ortega, A., Goebel, D., Becatti, G., "Dynamics of a Hollow Cathode Discharge in the Frequency Range of 1-500 kHz", Plasma Sources Science and Technology, in review, 2019